Research Article

Inhibition of Ataxia Telangiectasia Mutated Kinase Activity Enhances TRAIL-Mediated Apoptosis in Human Melanoma Cells

Vladimir N. Ivanov,[1] Hongning Zhou,[1] Michael A. Partridge,[1] and Tom K. Hei[1,2]

[1]Center for Radiological Research, College of Physicians and Surgeons, and [2]Department of Environmental Health Sciences, Columbia University, New York, New York

Abstract

The aim of the present study was to elucidate the effects of ataxia telangiectasia mutated (ATM) kinase on the regulation of the extrinsic tumor necrosis factor-related apoptosis-inducing ligand (TRAIL) receptor 2/DR5-mediated death pathway in human melanoma cells. We revealed that total ATM protein levels were high in some human melanoma lines compared with normal cells. The basal levels of active form ATM phospho-Ser^{1981} were also detectable in many melanoma lines and could be further up-regulated by γ-irradiation. Pretreatment of several melanoma lines just before γ-irradiation with the inhibitor of ATM kinase KU-55933 suppressed p53 and nuclear factor-κB (NF-κB) activation but notably increased radiation-induced DR5 surface expression, down-regulated cFLIP (caspase-8 inhibitor) levels, and substantially enhanced exogenous TRAIL-induced apoptosis. Furthermore, γ-irradiation in the presence of KU-55933 rendered TRAIL-resistant HHMSX melanoma cells susceptible to TRAIL-mediated apoptosis. In addition, suppression of ATM expression by the specific short hairpin RNA also resulted in down-regulation of cFLIP levels, up-regulation of surface DR5 expression, and TRAIL-mediated apoptosis in melanoma cells. Besides p53 and NF-κB, crucial regulators of DR5 expression, transcription factor STAT3 is known to negatively regulate DR5 expression. Suppression of Ser^{727} and Tyr^{705} phosphorylation of STAT3 by KU-55933 reduced STAT3 transacting activity accompanied by elevation in DR5 expression. Dominant-negative STAT3β also efficiently up-regulated the DR5 surface expression and down-regulated cFLIP levels in melanoma cells in culture and *in vivo*. Taken together, our data show the existence of an ATM-dependent STAT3-mediated antiapoptotic pathway, which on suppression sensitizes human melanoma cells to TRAIL-mediated apoptosis. [Cancer Res 2009;69(8):3510–9]

Introduction

The nuclear protein kinase ataxia telangiectasia mutated (ATM) plays an important role in signaling the presence of DNA double-strand breaks to the cell cycle checkpoint machinery and to the DNA repair system (1). Furthermore, *ATM* deficiency results in neurodegeneration, immunodeficiency, and enhanced radiosensitivity, suggesting a crucial role for this gene in the regulation of cell proliferation and cell death (2). ATM, together with ATR, controls extensive protein networks encompassing >700 proteins that are responsive to DNA damage (3). The important targets of the ATM signaling pathways are transcription factors p53, nuclear factor-κB (NF-κB), ATF2, and STAT3, which are ultimately linked to regulation of the cell cycle and apoptosis (1, 4–6). Ionizing radiation and chemotherapy are the two main modalities for cancer treatment. The cytotoxic effects of many anticancer drugs and ionizing radiation are mediated through DNA damage resulting in the activation of DNA damage-induced cell signaling pathways, including activation of the ATM networks. In this scenario, ATM kinase plays a crucial role by balancing cell cycle arrest versus cell death (1).

The incidence of melanoma has substantially increased worldwide over the last 40 years. Most advanced melanomas respond poorly to radiotherapy and chemotherapy and no effective therapy exists to inhibit the metastatic spread of this cancer (7). Alternative therapies that have been suggested for inducing apoptosis in cancer cells are based on the direct activation of the extrinsic death signaling pathways using recombinant death ligands of the tumor necrosis factor superfamily, such as tumor necrosis factor-related apoptosis-inducing ligand (TRAIL), or agonistic monoclonal antibodies to TRAIL receptor (TRAIL-R) 2/DR5 and TRAIL-R1/DR4. TRAIL-R2 could often be found on the surface of different types of cancer cells, including melanoma cells, at higher expression levels compared with TRAIL-R1 (8). In contrast to normal cells, the expression of the decoy receptors TRAIL-R3 and TRAIL-R4 rarely occurred in human melanomas. Targeting TRAIL-R-mediated signaling pathways for induction of apoptosis is currently being evaluated in multiple clinical trials for several cancer types (9, 10). Finally, combined modality treatments, which may include γ-irradiation and stimulation of the TRAIL-R-mediated pathways, appear to be promising potential treatments to suppress cancer development (11–13). Because ATM activity is strongly up-regulated by γ-irradiation, we address the role of ATM in the regulation of apoptosis in human melanomas. The main aim of the present study was to resolve the question of how inhibition of ATM activity affected TRAIL-mediated extrinsic death pathway in human melanoma cells.

Materials and Methods

Materials. Human KILLER-TRAIL was purchased from Alexis. c-Jun NH_2-terminal kinase inhibitor SP600125 was obtained from Biomol. MEK inhibitor U0126, phosphatidylinositol 3-kinase inhibitor LY294002, IKK inhibitor BMS-345541, JAK2 inhibitor AG490, and ATM kinase inhibitor KU-55933 were purchased from Calbiochem.

Cell lines. Human melanoma cell lines LU1205 (also known as 1205lu), WM9, WM35 (14), and HHMSX and normal human fibroblasts TIG3 were maintained in DMEM supplemented with 10% fetal bovine serum, L-glutamine, and antibiotics. Normal human lung fibroblasts (MRC5) and human ATM-deficient fibroblasts (GM02052) were obtained from Coriell Cell Repository. These cells were maintained in Eagle's MEM supplemented with 15% fetal bovine serum, vitamins, amino acids, and antibiotics.

Note: Supplementary data for this article are available at Cancer Research Online (http://cancerres.aacrjournals.org/).

Requests for reprints: Vladimir N. Ivanov, Center for Radiological Research, Columbia University, VC11-236, 630 West 168th Street, New York, NY 10032. Phone: 212-305-9667; Fax: 212-305-3229; E-mail: vni3@columbia.edu.

doi:10.1158/0008-5472.CAN-08-3883

Irradiation procedures. To determine sensitivity to γ-rays, the plates with melanoma cells were exposed to radiation from a Gammacell 40 ^{137}Cs irradiator.

Fluorescence-activated cell sorting analysis of DR5 and FAS levels. Surface levels of DR5 and FAS were determined by staining with the phycoerythrin-labeled monoclonal antibodies from eBioscience and BD Biosciences. A FACSCalibur flow cytometer (Becton Dickinson) combined with the CellQuest program was used to perform flow cytometric analysis.

Transfection and luciferase assay. The NF-κB luciferase reporter containing two κB-binding sites, Jun2-Luc reporter (15), and the STAT-Luc reporter containing three repeats of GAS sites were used to determine NF-κB, AP-1, and STAT transactivation, respectively. Additional reporter constructs used included DR5/TRAIL-R2-full-Luc, which contained 1.6 kb upstream of the ATG site through intron 2 in the DR5 genomic locus (16), a 1 kb cFLIP-promoter-Luc (17, 18), and p53RE-Luc (19). Transient transfection of reporter constructs (1 μg) together with pCMV-β-galactosidase (0.25 μg) into 5×10^5 melanoma cells was done using Lipofectamine (Life Technologies). Luciferase activity was determined using the luciferase assay system (Promega) and was normalized based on β-galactosidase levels.

Mutational analysis of DR5 promoter. Mutations within the STAT-binding site of the human TRAIL-R2/DR5 promoter and within the κB site of the intron 2 were generated using DR5/TRAIL-R2-full-Luc construct (16) and the QuikChange kit (Stratagene).

Suppression of ATM expression with short hairpin RNA. ATM expression in melanoma cells was stably knocked down using pRetroSuper constructs with short hairpin RNA (shRNA) sequences corresponding to positions 912 (ATM1) and 8,538 (ATM3) of the ATM transcript. Green fluorescent protein (GFP) shRNA served as a mock control. These constructs have been kindly provided by Dr. Y. Shiloh (20). LU1205 melanoma cells were transfected by shRNA constructs using Lipofectamine and selected with 0.5 μg/mL puromycin.

Apoptosis studies. Cells were exposed to soluble TRAIL (50 ng/mL) alone or in combination with cycloheximide (2 μg/mL). Different variants of combined treatment were used, including γ-irradiation (5 Gy), in the presence or absence of specific inhibitors of signaling pathways followed by TRAIL treatment. Apoptosis was then assessed by quantifying the percentage of hypodiploid nuclei using fluorescence-activated cell sorting analysis.

Western blot analysis. Total cell lysates (50 μg protein) were resolved on SDS-PAGE and processed according to standard protocols. The monoclonal antibodies used for Western blotting included anti-β-actin (Sigma); anti-FLIP (NF6; Axxora); anti-caspase-3 and -8; anti-ATM (D2E2) and anti-phospho-ATM (Ser^{1981}); anti-phospho-p53 (Ser^{15}; Cell Signaling); and anti-X-linked inhibitor of apoptosis protein (XIAP; clone 48; BD Biosciences). The polyclonal antibodies used included anti-TRAIL and anti-DR5 (Axxora); anti-phospho-p53 (Ser^{20}) and anti-total p53; anti-phospho-SAPK/c-Jun NH_2-terminal kinase (JNK; Thr^{183}/Tyr^{185}) and anti-JNK; anti-phospho-p44/p42 mitogen-activated protein kinase (Thr^{202}/Tyr^{204}) and anti-p44/p42 mitogen-activated protein kinase; anti-phospho-AKT (Ser^{473}) and anti-AKT; anti-poly(ADP-ribose) polymerase; anti-STAT3, anti-phospho-STAT3 (Tyr^{705}) and anti-phospho-STAT3 (Ser^{727}); and anti-Chk2 and anti-phospho-Chk2 (Thr^{68}; Cell Signaling). The secondary antibodies were conjugated to horseradish peroxidase; signals were detected using the enhanced chemiluminescence system (Amersham).

Electrophoretic mobility shift assay. Electrophoretic mobility shift assay was done for the detection of NF-κB DNA-binding activity as described previously. Ubiquitous NF-Y DNA-binding activity was used as an internal control (21).

Human melanoma transplant in nude mice. LU1205 cells (1×10^6) stably transfected with control empty vector pBabe-puro or with STAT3β expression construct were injected subcutaneously into 7-week-old athymic nude mice BALB/c *nu/nu* (6 mice per group) obtained from The Jackson Laboratory. Tumor growth was monitored every 2 days. Three weeks after beginning of the experiments, the tumor were excised, weighted, and subjected to histopathologic and immunochemical examination.

Statistical analysis. Data were calculated as mean and SD. Comparisons of results between treated and control groups were made by the Students' *t* tests. $P \leq 0.05$ between groups was considered significant.

Results

ATM levels and DR5 surface expression in human melanoma cell lines. Two primary human fibroblast lines, MRC5 (*ATM*+/+) and GM02052 (*ATM*−/−), were used as positive and negative controls, respectively, for comparing the expression levels of ATM protein and its signaling pathways in human melanoma cells (Fig. 1*A* and *B*). Autophosphorylation of ATM after γ-irradiation (22), with the subsequent ATM-Chk2-dependent phosphorylation of p53-Ser^{20} (23) that are characteristic features of the ATM signaling pathway, are clearly deficient in *ATM*−/− fibroblast line (Fig. 1*A*). In contrast to normal fibroblasts MRC5, human melanoma lines were characterized by increased protein levels of both total ATM and its active form, ATM phospho-Ser^{1981} (Fig. 1*B*). Basal p53 protein levels in melanoma lines were also correlated to ATM protein levels. ATM levels in human melanocytes were similar to levels in human fibroblasts (data not shown).

Numerous human melanoma lines express TRAIL-R2/DR5 on their surface (12, 24). In contrast, surface expression of TRAIL-R1/DR4 was found at marginal levels in many melanoma lines (Supplementary Fig. *S1*). The remarkable exceptions were the early melanomas WM1552C and SBcl2 (25) as well as ocular melanoma OM431 (26), which exhibited the increased levels of surface DR4. Interestingly, surface expression of DR5 in WM9 and LU1205 melanoma cells was substantially higher than in HHMSX melanoma cells, showing an inverse correlation between the basal ATM levels and DR5 surface expression (Fig. 1*B* and *C*). Both MRC5 (*ATM*+/+) and GM02052 (*ATM*−/−) fibroblasts contained two cell subpopulations with zero and moderate levels of DR5 on the cell surface, respectively. Although GM02052 cells had a modest increase in the percentage of DR5-positive cells (58%) compared with MRC5 (35%; Fig. 1*C*), the different genetic background of these cell lines did not allow us to make a definite conclusion concerning quantitative effects of ATM on the DR5 surface expression in fibroblasts. However, these data show that, in the case of ATM deficiency, moderate levels of the DR5 surface expression are observed in fibroblasts. Interestingly, ATM deficiency did not change the levels of surface FAS in fibroblasts (Fig. 1*C*). Next, we used pRetroSuper constructs expressing ATM1 and ATM3 shRNA for stable suppression of ATM levels and GFP shRNA as a mock control (20) in MRC5 cells. ATM1 shRNA caused ~70% decrease in total ATM protein levels of MRC5 cells that was accompanied by modest increase in DR5 surface expression (Fig. 1*D*), indicating a negative role of ATM in regulation of DR5 expression.

TRAIL-R2/DR5 gene expression is a target for positive regulation by γ-irradiation in many cancer cell lines (27). Indeed, DR5 total and surface levels and activity of the *DR5* promoter were further increased 6 to 16 h after irradiation of LU1205 cells, whereas, for MRC5 and GM02052 fibroblasts, up-regulation of the surface DR5 expression was not pronounced (Figs. 1*C* and 2*B* and *C*). Because activation of ATM kinase by DNA damage after γ-irradiation is involved in the up-regulation of the p53 and NF-κB pathways (28), a role for ATM kinase in the regulation of *DR5* gene expression, levels of NF-κB-dependent antiapoptotic proteins, and TRAIL-mediated apoptosis in melanoma cells was further investigated in this study.

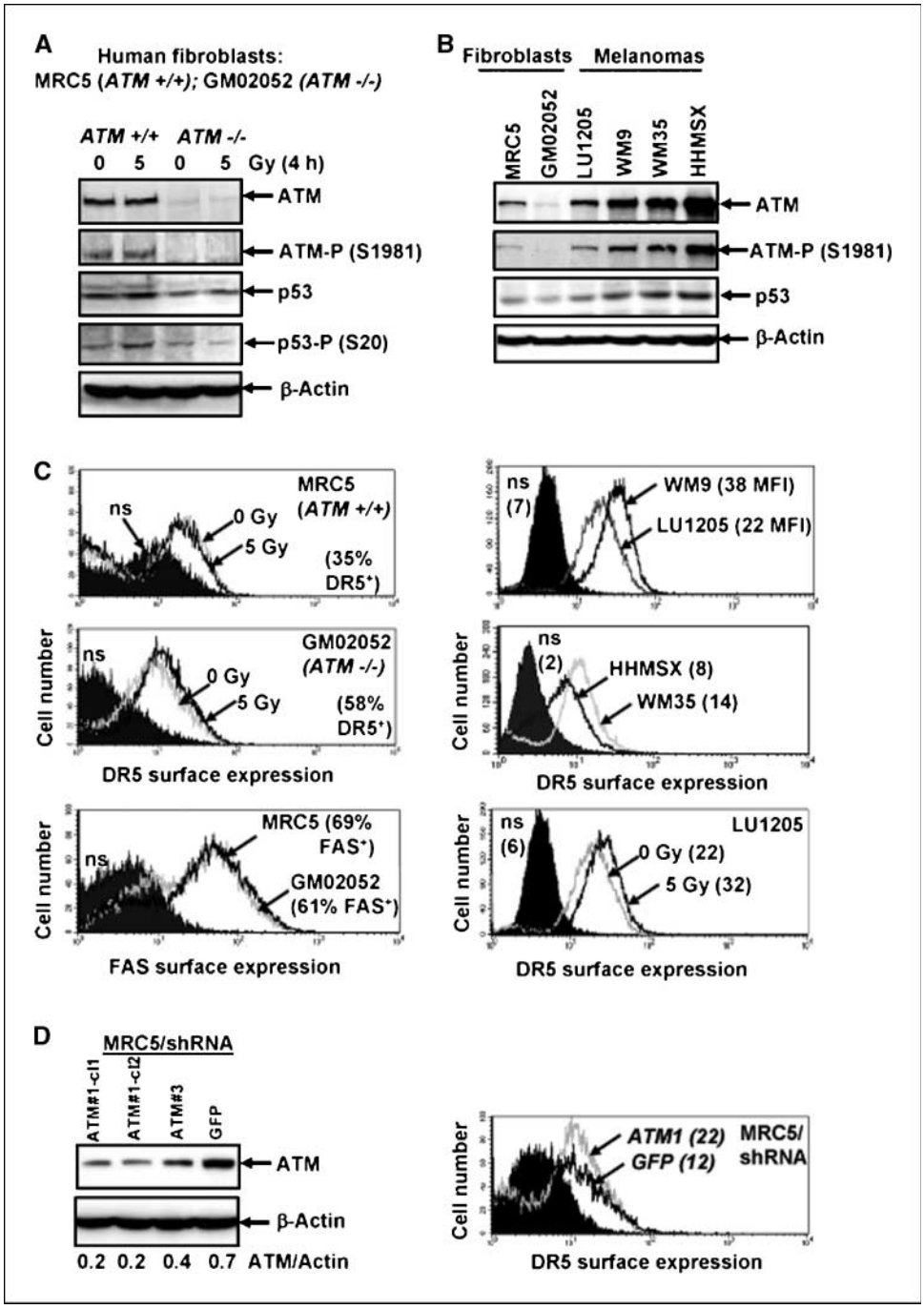

Figure 1. ATM levels and TRAIL-R2/DR5 surface expression in human fibroblast and melanoma lines. *A,* Western blot analysis of total ATM, ATM phospho-Ser^{1981} [*ATM-P (S1981)*], total p53, and p53 phospho-Ser^{20} [*p53-P (S20)*] in MRC5 (*ATM*+/+) and GM02052 (*ATM*−/−) human fibroblasts before and 4 h after γ-irradiation (5 Gy). *B,* Western blotting of indicated proteins in fibroblast and melanoma lines. Actin served as a control of protein loading. *C,* surface expression of DR5 and FAS in fibroblast and melanoma lines was determined before and 16 h after γ-irradiation using fluorescence-activated cell sorting analysis. Median fluorescence intensity (*MFI*) is indicated for melanoma cells. *D,* MRC5 cultures permanently transfected with pRetroSuper constructs expressing shRNA for GFP (mock control), ATM1, and ATM3 were established. Western blotting showed ATM and β-actin levels. Surface DR5 expression (MFI) increased in ATM-deficient cells.

Inhibition of ATM kinase in γ-irradiated melanoma cells reduced p53 and NF-κB activities and cFLIP levels. γ-Irradiation of LU1205 cells induced autophosphorylation and up-regulation of ATM kinase activity in a dose-dependent manner (Fig. 2*A*) that was accompanied by further activation of Chk2 and Chk2-mediated Ser^{20} phosphorylation of p53. On the other hand, direct ATM-mediated Ser^{15} phosphorylation of p53 was observed at low levels. KU-55933 (10 μmol/L), a specific inhibitor of ATM kinase activity (29), suppressed ATM autophosphorylation after irradiation and caused down-regulation of p53 phospho-Ser^{20} levels (Fig. 2*B*) and NF-κB DNA-binding activity (Fig. 2*C*), which was accompanied by a decrease of general p53- and NF-κB-dependent gene expression in the irradiated cells (Fig. 2*C*). KU-55933 was less effective for inhibition of the basal NF-κB activity compared with BMS-345541 (20 μmol/L), a specific inhibitor of IKK-NF-κB. Both inhibitors were equally effective in the suppression of the radiation-induced NF-κB activity (Fig. 2*C*). Luciferase assay also showed down-regulation of the cFLIP promoter activity with KU-55933 (Fig. 2*C*), which was accompanied by decrease in cFLIP-S and cFLIP-L protein levels detected by Western blotting 8 h after treatment with KU-55933 in both nonirradiated and γ-irradiated cells (Fig. 2B). In contrast, the DR5 promoter activity and total DR5 protein levels modestly increased 4 to 6 h after irradiation, especially in the presence of KU-55933 (Fig. 2*B* and *C*). The

observed decrease in p53 and NF-κB activities following inhibition of ATM kinase activity by KU-55933 in γ-irradiated cells correlated with a substantial up-regulation of G_2-M arrest of the cell cycle. This was likely due to a failure to arrest in S phase (29, 30), a characteristic feature of ATM deficiency in both LU1205 melanoma cells and TIG3 human fibroblasts. KU-55933 up-regulated levels of G_2-M arrest in irradiated normal TIG3 fibroblasts were higher compared with treated cancer cells (Fig. 2*D*).

Inhibition of ATM activity increased the sensitivity of melanoma cells to TRAIL-mediated apoptosis. DNA repair mechanisms might permit the cells to overcome the consequences of the DNA damage. However, suppression of ATM activity after γ-irradiation in the presence of KU-55933 could exert an alternative effect on the apoptotic machinery in the cells via regulation of expression of the components of the extrinsic apoptotic pathway. KU-55933 efficiently up-regulated TRAIL-mediated apoptosis of LU1205 and WM35 cells (Fig. 3*A* and *D*), probably due to down-regulation of cFLIP levels, which was quite similar to cFLIP-RNA interference-mediated suppression of cFLIP and the subsequent up-regulation of TRAIL-induced apoptosis in melanoma cells (24). Down-regulation of basal cFLIP protein levels by KU-55933 was dependent on down-regulation of *cFLIP* gene expression (Fig. 2*C*) followed by proteasome-dependent degradation of cFLIP and could be blocked with the proteasome inhibitor, MG132 (data not shown). On the other hand, cleavage of procaspase-8 and procaspase-3 and the caspase-3-mediated cleavage of poly(ADP-ribose) polymerase and XIAP p57 were well pronounced 6 h after treatment by a combination of KU-55933 and TRAIL. XIAP p57 and cFLIP levels were also effectively down-regulated by treatment with TRAIL alone via caspase cascade (Fig. 3*A*). A detailed analysis of cFLIP-L levels after treatment with KU-55933 or TRAIL in the presence or absence of a universal caspase inhibitor, zVAD-fmk, and a specific inhibitor of caspase-8, Ac-IETD-CHO, was also performed (Supplementary Fig. *S2*). Results obtained clearly showed a caspase-independent down-regulation of cFLIP levels 2 to 4 h after treatment with KU-55933 and caspase-dependent down-regulation

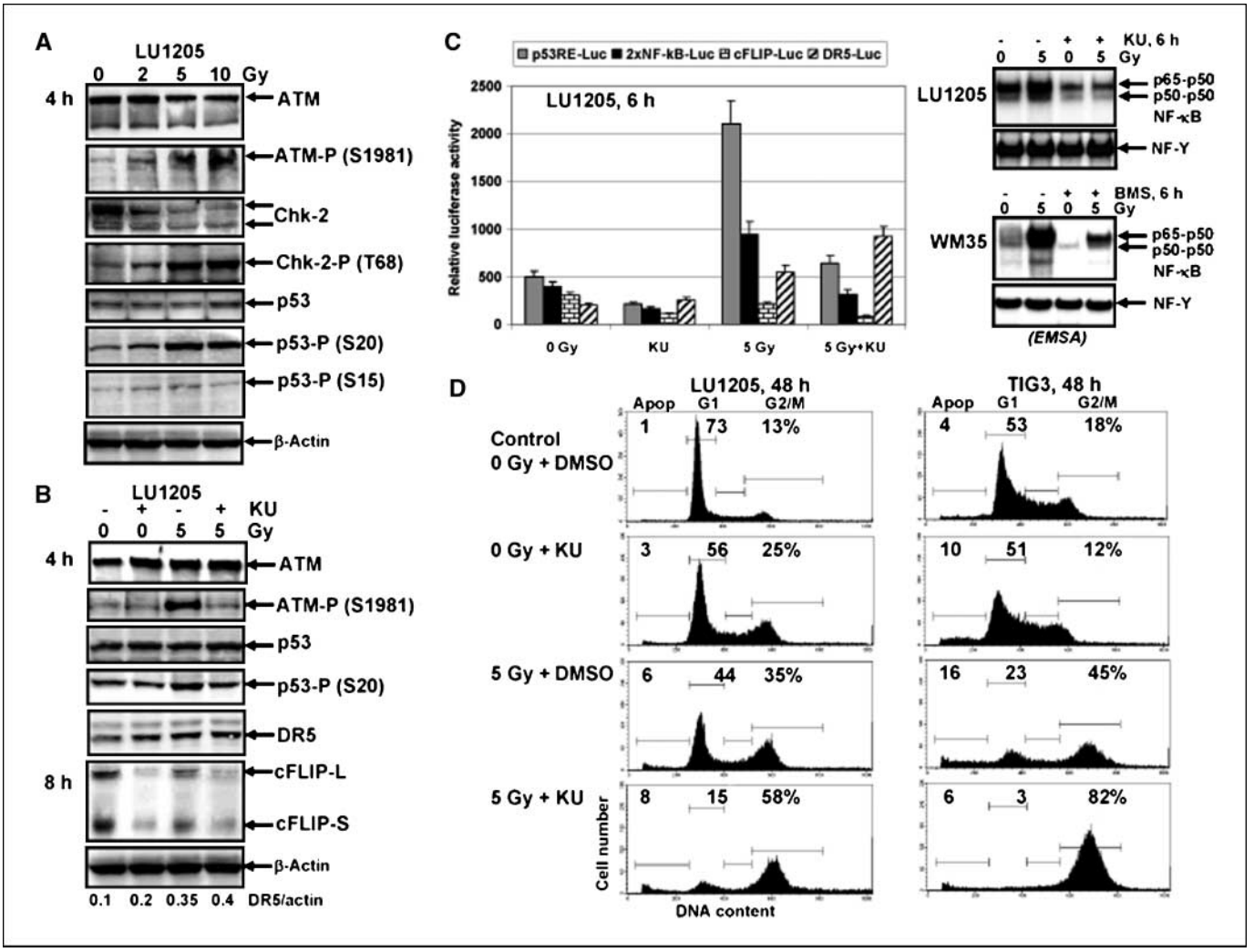

Figure 2. Suppression of ATM activity by KU-55933 increased G_2-M cell cycle arrest after γ-irradiation. *A* and *B,* Western blotting of indicated proteins in LU1205 cells 4 or 8 h after γ-irradiation in the presence or absence of KU-55933 (*KU*; 10 μmol/L). Actin served as a protein loading control. *C,* effects of γ-irradiation (5 Gy) and KU-55933 (10 μmol/L) on NF-κB– and p53-dependent luciferase reporter activities and on cFLIP and DR5 promoter activities 6 h after treatment. *Columns,* mean; *bars,* SD ($P < 0.05$, Student's *t* test). Electrophoretic mobility shift assay of nuclear NF-κB activity in LU1205 and WM35 cells 6 h after γ-irradiation in the presence or absence of KU-55933 (10 μmol/L) and BMS-345541 (20 μmol/L). Positions of two NF-κB DNA-binding complexes are indicated. Ubiquitous NF-Y DNA-binding complex was used as an internal control. *D,* cell cycle analysis of LU1205 melanoma cells and TIG3 fibroblasts 48 h after treatment using flow cytometry. KU-55933 in 0.1% DMSO that was added 0.5 h before γ-irradiation.

6 h after treatment. Hence, the initial decrease in cFLIP-L levels after treatment with KU-55933 was not a result of apoptosis, whereas the late decrease in cFLIP-L levels was indeed a consequence of apoptosis. Levels of apoptosis determined 48 h after treatment were substantially higher for a combination of TRAIL and KU-55933 than for TRAIL alone (Fig. 3*D*).

Efficacy of TRAIL-mediated apoptosis could be further increased through radiation-induced up-regulation of the total and surface DR5 expression (12), which was positively controlled by p53 and NF-κB (16, 31). As expected, BMS-345541, a specific inhibitor of the IKK-NF-κB pathway, suppressed NF-κB activation in melanoma cells (Fig. 2*C*) and prevented radiation-induced up-regulation of DR5 surface expression in WM35 and LU1205 cells (Fig. 3*B*). Given the positive role for NF-κB and p53 in regulation of *DR5* transcription (16, 31, 32), it was quite unexpected, however, that instead of suppression of *DR5* expression, we observed an additional up-regulation of the *DR5* promoter activity (Fig. 2*C*) and DR5 surface expression after γ-irradiation in the presence of KU-55933 (10 μmol/L) in four melanoma lines, WM35, LU1205, WM9, and HHMSX (Fig. 3*B*; data not shown).

Hence, pretreatment of LU1205 and WM35 cells with γ-irradiation that up-regulated the total and surface expression of DR5 (Fig. 3*B*), especially in the presence of KU-55933, further increased levels of TRAIL-mediated apoptosis (Fig. 3*D*). On the other hand, IKK-NF-κB inhibitor BMS-345541 decreased apoptotic levels after irradiation of melanoma cells (Fig. 3*D*), correlating with decreased levels of NF-κB-dependent proapoptotic DR5 after irradiation in the presence of BMS-345541. In contrast to DR5, radiation-induced surface FAS expression in LU1205 cells was not further increased in the presence of KU-55933 (Fig. 3*C*).

KU-55933 sensitizes resistant HHMSX melanoma cells to TRAIL-mediated apoptosis. Additional experiments showed that up-regulation of DR5 surface levels and down-regulation of cFLIP protein levels after irradiation in the presence of KU-55933 (data

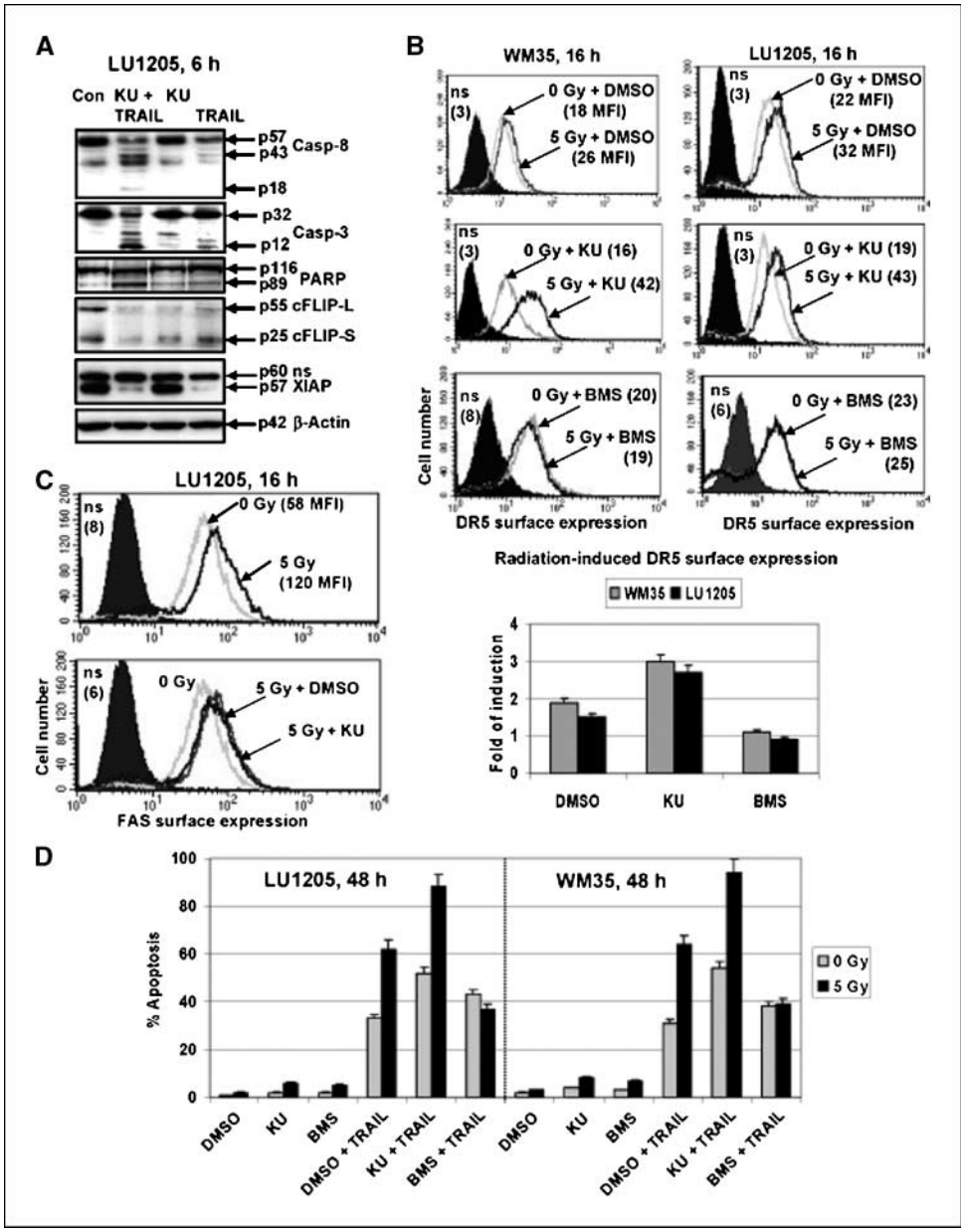

Figure 3. KU-55933 increased DR5 surface expression and TRAIL-mediated apoptosis of γ-irradiated LU1205 and WM35 melanoma cells. *A,* Western blot analysis of caspase-8 (*Casp-8*), caspase-3 (*Casp-3*), and poly(ADP-ribose) polymerase (*PARP*) cleavage, XIAP, cFLIP-L, cFLIP-S, and β-actin levels following treatment of LU1205 cells by TRAIL (50 ng/mL), KU-55933 (10 μmol/L), or their combination. Band p60 determined by anti-XIAP monoclonal antibody (clone 48) was nonspecific. *B* and *C,* surface expression of DR5 and FAS in LU1205 and WM35 cells 16 h after irradiation (5 Gy). KU-55933 and BMS-345541 (*BMS*) were added to medium 0.5 h before irradiation. Results of a typical experiment with WM35 and LU1205 cells are shown in *B* (*top*). Radiation-induced levels of DR5 surface expression in the presence of DMSO, KU-55933, or BMS-345541 normalized to DR5 levels before irradiation are shown in *B* (*bottom*). *Columns,* mean; *bars,* SD. *D,* LU1205 and WM35 cells were γ-irradiated in the presence of DMSO, KU-55933, or BMS-345541. Sixteen hours after irradiation, cells were treated with TRAIL (50 ng/mL) for an additional 32 h. Apoptosis levels were determined as the percentage of cells with hypodiploid content of DNA using flow cytometry. *Columns,* mean of four independent experiments; *bars,* SD ($P < 0.05$, Student's *t* test).

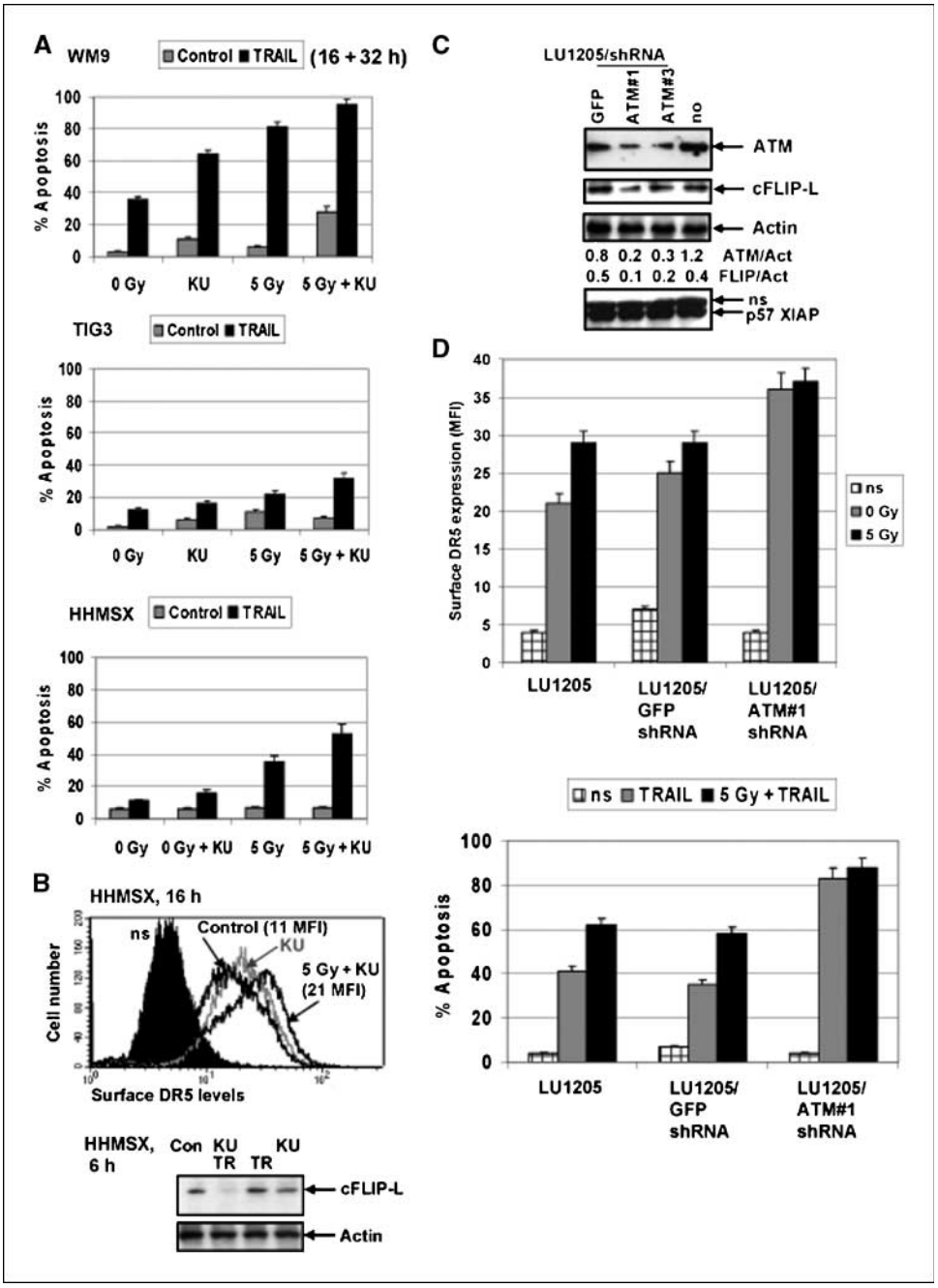

Figure 4. Inhibition of ATM activity by KU-55933 or down-regulation of ATM levels by specific shRNA increased DR5 surface expression and TRAIL-mediated apoptosis in melanoma cells. *A,* indicated cell lines were γ-irradiated in the presence or absence of KU-55933. Eighteen hours after irradiation, cells were treated with TRAIL (50 ng/mL) for an additional 32 h. Apoptosis levels were determined as the percentage of cells with hypodiploid content of DNA. *Columns,* mean; *bars,* SD. *B,* DR5 surface levels of HHMSX cells after treatments with DMSO, KU-55933, or 5 Gy + KU-55933 were determined by flow cytometry. Western blotting showed cFLIP levels 6 h after treatment of HHMSX cells with TRAIL (*TR*) and KU-55933. *C,* LU1205 mass cultures permanently transfected with pRetroSuper constructs expressing shRNA for GFP (mock control), ATM1, and ATM3 were established. Western blotting showed ATM, cFLIP-L, and XIAP levels in these cultures. *D,* surface DR5 expression (MFI) and apoptosis levels in indicated cultures. *Columns,* mean; *bars,* SD ($P < 0.05$, Student's *t* test).

not shown) was accompanied by accelerated TRAIL-mediated apoptosis in WM9 melanoma cells. In contrast, TRAIL-mediated apoptosis of TIG3 normal fibroblasts was substantially lower (Fig. 4*A*) based probably on a protective mechanism for TRAIL-mediated apoptosis in normal cells. We used the similar treatment for up-regulation of TRAIL-mediated apoptosis in resistant HHMSX melanoma cells (Fig. 4*A*). Besides low surface expression of DR5 (Fig. 1*D*), these cells were characterized by notably suppressed mitochondrial function (24). KU-55933 alone, but not TRAIL, caused only modest down-regulation of cFLIP-L levels in these cells (Fig. 4*B*). The sequential treatment of these cells initially with a combination of KU-55933 and γ-radiation that up-regulated DR5 surface levels (Fig. 4*B*) and then with recombinant TRAIL (50 ng/mL) in the presence of KU-55933 (10 μmol/L) that additionally decreased cFLIP levels (Fig. 4*B*) induced pronounced apoptosis showing a sensitization to TRAIL.

ATM suppression by shRNA. We used pRetroSuper constructs expressing ATM1 and ATM3 shRNA for stable suppression of ATM and GFP shRNA as a mock control (20) in melanoma cells. After selection in the presence of puromycin, LU1205 mass cultures expressing ATM1, ATM3, and GFP shRNA were obtained. ATM3 and especially ATM1 shRNA were effective in the suppression of total ATM levels. ATM1 shRNA caused ~75% decrease in total ATM protein levels of LU1205 cells (Fig. 4*C*). ATM down-regulation was accompanied by an increase in the percentage of G_2-M arrested cells 48 h after irradiation (5 Gy) of the ATM-deficient culture in comparison with the percentage in the irradiated control culture (18-34%; data not shown). Furthermore, we observed in

ATM-deficient cells a partial suppression of the basal cFLIP-L, but not XIAP, protein levels and a notable up-regulation of DR5 surface expression, which did not further increase after γ-irradiation (Fig. 4*D*). TRAIL-induced apoptosis was maximal in LU1205/ATM1 cells compared with the control cells (Fig. 4*D*). Results obtained with suppression of ATM expression by specific shRNA generally confirmed our data based on an inhibition of ATM activity by its inhibitor KU-55933 (see Fig. 3). However, certain differences between these two approaches have also been observed. Irradiation had no additional effect on DR5 surface expression in ATM-deficient cells compared with untreated ATM-deficient cells with already increased DR5 expression (Fig. 4*D*), whereas irradiated and KU-55933-treated cells showed higher DR5 expression than KU-55933-treated nonirradiated cells (Fig. 4*A*). Consequently, there was no additional increase in levels of TRAIL-mediated apoptosis in ATM-deficient irradiated cells compared with already high levels of TRAIL-mediated apoptosis in nonirradiated ATM-deficient cells (Fig. 4*D*). Such differences are probably results of a substantial change in the basal characteristics of ATM-deficient cells. However, the critical feature, pronounced up-regulation of TRAIL-mediated apoptosis in melanoma cells, was observed for both approaches.

Role of STAT3 Tyr^{705} and Ser^{727} phosphorylation in ATM-dependent regulation of DR5 expression. Several signaling pathways and the corresponding transcription factors may be involved in the regulation of radiation-induced DR5 expression: ATM-Chk2-p53, IKK-NF-κB, MEK-extracellular signal-regulated kinase (ERK)-Elk1, MKK4/7-JNK-cJun, and JAK2-STAT3. Because suppression of p53 and NF-κB activities by KU-55933 was not accompanied by a decrease in the DR5 surface expression, it might indicate the existence of an alternative ATM-dependent signaling pathway,

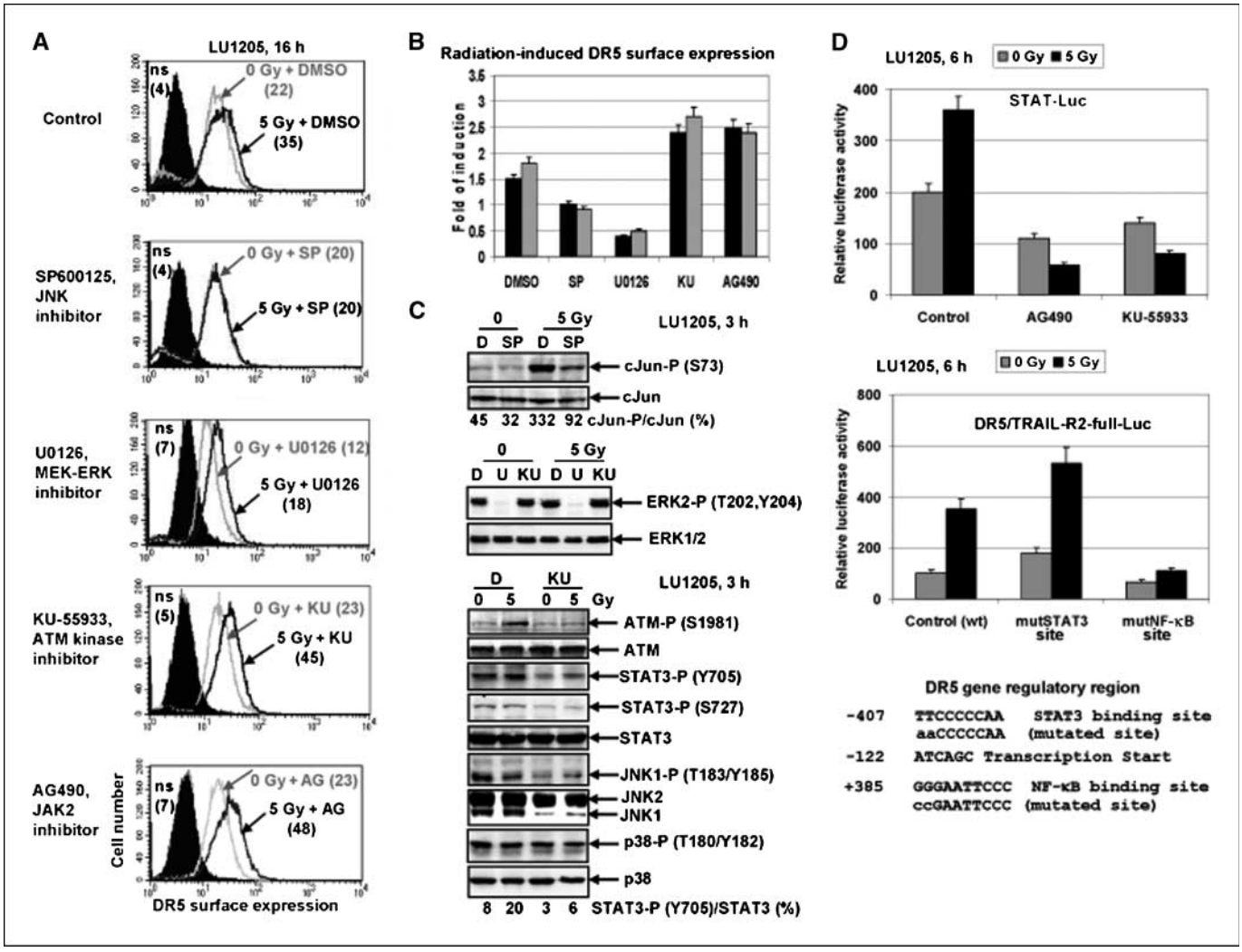

Figure 5. Effects of specific inhibition of signaling pathways on DR5 surface expression in LU1205 cells. *A* and *B,* LU1205 cells were γ-irradiated in the presence of DMSO, SP600125 (10 μmol/L), U0126 (10 μmol/L), AG418 (50 μmol/L), or KU-55933 (10 μmol/L). Surface expression of DR5 in melanoma cells was determined 16 h after irradiation (5 Gy). Results of a typical experiment are presented in *A*. Radiation-induced levels of DR5 surface expression in the presence DMSO, SP600125 (*SP*), U0126, KU-55933, or AG490 (*AG*) normalized to DR5 levels before treatment are shown in *B. Columns,* mean; *bars,* SD ($P < 0.05$, Student's *t* test). *Black columns,* LU1205; *grey columns,* WM35 cells. *C,* Western blotting of total and phosphorylated protein levels of c-Jun, ERK, ATM, STAT3, JNK, and p38 in LU1205 cells after indicated treatment. DMSO (*D*), U0126 (*U*), and KU-55933 (*KU*) were added 30 min before irradiation. A ratio STAT3 phospho-Tyr^{705} [*STAT3-P (Y705)*]/total STAT3 (%) is indicated. *D,* effects of AG490 and KU-55933 on STAT-dependent reporter activity before and after γ-irradiation (5 Gy). A role of STAT3-binding site for the *DR5* promoter activity. Positions of the transcription start and the STAT3 and NF-κB-binding sites are indicated. Transient transfection of the control (*wt*) DR5/TRAIL-R2-full-Luc reporter as well as constructs with the mutated STAT3- or NF-κB-binding site was done using LU1205 cells. Sixteen hours after transfection, cells were irradiated and normalized luciferase activity was determined 6 h after treatment.

characterized by the activation of a transcription factor that could negatively control DR5 expression.

We used specific inhibitors of signaling pathways to further resolve the mechanism of regulation of DR5 expression. Similarly to the inhibitor of IKK-NF-κB (Fig. 3*B*), JNK inhibitor SP600125 (10 μmol/L) blocked an increase in DR5 surface expression (Fig. 5*A* and *B*). As expected, this inhibitor down-regulated c-Jun phosphorylation (Fig. 5*C*) after γ-irradiation of LU1205 cells. These results indicated a positive role of JNK in the regulation of radiation-induced DR5 expression (Fig. 5*A* and *B*) that further confirmed observations on the significance of JNK-SP1 for enhancing expression of DR5 (33). U0126 (10 μmol/L), a MEK-ERK inhibitor, substantially decreased DR5 surface expression in both nonirradiated and irradiated cells (Fig. 5*A* and *B*). This inhibitor suppressed constitutive ERK1/2 phosphorylation in LU1205 cells, whereas KU-55933 had no effects (Fig. 5*C*). Only AG490 (50 μmol/L), a JAK2-STAT3 inhibitor, resembled the positive effects of KU-55933 on DR5 levels in melanoma cells (Fig. 5*A* and *B*). STAT3 Tyr^{705} phosphorylation mediated by JAK2 is involved in STAT3 dimerization and its subsequent translocation to the nucleus and interaction with genomic DNA (34). Ser^{727} phosphorylation of STAT3 further increases STAT3 transacting functions in the gene promoters.

KU-55933 treatment, as expected, suppressed radiation-induced ATM activation and notably reduced basal and radiation-induced levels of both STAT3 Tyr^{705} and Ser^{727} phosphorylation (Fig. 5*C*). A luciferase assay confirmed the summary negative effects of KU-55933 on STAT3-dependent reporter activity in γ-irradiated cells that was quite similar to STAT3-Luc inhibition by AG490 (Fig. 5*D*). A role of ATM, as well as the mitogen-activated protein kinase and mammalian target of rapamycin pathways in Ser^{727} phosphorylation of STAT3, was previously established (6, 34), whereas the ATM-dependent pathway that affects tyrosine phosphorylation of STAT3 is currently unknown. Interestingly, KU-55933 also partially suppressed JNK1 but not p38 phosphorylation, which might be a reason for the decrease in Ser^{727} phosphorylation of STAT3 via JNK1 (Fig. 5*C*). Our data indicated an up-regulation of DR5 total and surface expression upon suppression of phospho-Tyr^{705}- and phospho-Ser^{727}-dependent STAT3 functions, which was consistent with suggestion on STAT3 to be a negative regulator of DR5 expression and TRAIL-mediated apoptosis (35, 36). To further confirm a negative regulation of DR5 expression by STAT3, we mutated the STAT3-binding site in the DR5 promoter using a site-directed mutagenesis kit (QuikChange; Stratagene). This resulted in pronounced up-regulation of the DR5-luciferase activity before and after γ-irradiation, whereas mutations in the intronic NF-κB-binding site resulted in a down-regulation of DR5-luciferase activity (31) in melanoma cells (Fig. 5*D*).

Dominant-negative STAT3β substantially increased DR5 surface expression on melanoma cells both in cell culture and *in vivo*. Next, we used previously established melanoma lines LU1205 stably transfected with the empty vector (pBabe-puro) or by STAT3β, a dominant-negative form of STAT3 with the 55-amino acid COOH-terminal deletion, including Ser^{727}, which strongly suppressed STAT3 transcriptional activity (37, 38). STAT3β overexpression moderately decreased cell growth in culture and strongly increased surface expression of DR5 in both nontreated and irradiated LU1205 melanoma cells (Fig. 6*A* and *B*). Furthermore, LU1205/STAT3β cells contained a decreased basal level of cFLIP-L and cFLIP-S compared with the control cells (Fig. 6*A*). Taken together, this correlated with increased TRAIL-mediated apoptosis in STAT3β-transfected LU1205 cells (Fig. 6*C*). We next examined whether STAT3β-dependent up-regulation of the DR5 surface expression was maintained *in vivo*. Interestingly, the LU1205-STAT3β melanoma xenotransplant exhibited a dramatic decrease in tumor volume compared with the control LU1205-puro transplant in athymic nude mice 3 weeks after injection of melanoma cells (Fig. 6*D*). The DR5 surface expression was maintained notably higher in LU1205-STAT3β tumor cells *in vivo* than in the control LU1205-puro tumors (Fig. 6*D*). Taken together, these data confirmed that suppression of ATM-dependent STAT3 activation enhanced TRAIL-mediated apoptosis through up-regulation of surface DR5 expression, whereas suppression of both STAT3 and NF-κB appeared to be involved in down-regulation of cFLIP (see Figs. 2*B*, 3*A*, and 6*A*) accompanied by an additional increase in apoptotic levels.

In general, the ATM inhibitor KU-55933 affected TRAIL-mediated apoptosis more strongly than the JAK2 inhibitor, AG490, or overexpression of STAT3β (Fig. 6*C*). Finally, LY294002 (50 μmol/L), a universal inhibitor of phosphatidylinositol 3-kinase and phosphatidylinositol 3-kinase-like kinases, including ATM, induced the strongest acceleration of TRAIL-mediated apoptosis in melanoma cells (Fig. 6*C*), indicating for a role of other members of this family in suppression of TRAIL-mediated apoptosis. A combination of KU-55933 and LY294002 did not additionally increase levels of TRAIL-induced apoptosis compared with apoptosis in the presence of LY294002 alone. Hence, the ATM pathway regulated antiapoptotic function in melanoma cells that substantially suppressed TRAIL-mediated apoptosis.

Discussion

A role for the suppression of ATM activity in sensitizing cancer cells to radiation-induced death was already described (39, 40). Consequently, targeted cancer therapy based on the inhibition of DNA strand break repair is currently being undertaken in numerous clinical trials (41). As most metastatic melanomas are radioresistant, ionizing radiation alone is rarely used for treatment of this disease. We investigated in the present study an alternative approach involving a combined treatment of γ-irradiation and an inhibitor of ATM kinase followed by induction of recombinant TRAIL-mediated apoptosis. Using inhibition of ATM activity by KU-55933 or a partial suppression of ATM expression by specific ATM shRNA stably transfected in melanoma cells, we observed a substantial up-regulation of TRAIL-mediated apoptosis.

A previous report described ATM-dependent activation of STAT3 transcriptional activity (6) that might negatively control DR5 gene expression, which we confirmed in the present study. Consequently, partial reduction of Ser^{727} and Tyr^{705} phosphorylation of STAT3 by KU-55933 reversed DR5 down-regulation, which was directed by ATM. A role for ATM, mammalian target of rapamycin, and the mitogen-activated protein kinase pathways in Ser^{727} phosphorylation of STAT3 was described previously (6, 34), whereas an ATM-dependent signaling pathway resulting in up-regulation of tyrosine phosphorylation of STAT3 needs to be investigated. Further, dominant-negative STAT3β with deleted Ser^{727} was effective in several actions, such as suppression of melanoma xenotransplant growth, probably via inhibition of STAT3-dependent expression of cyclin D1 (42), and an up-regulation of DR5 and FAS (37) surface expression in cell culture and *in vivo*. A substantial inhibition of melanoma xenotransplant growth by STAT3β might also indicate a role for DR5- and FAS-mediated apoptosis in this process.

A negative role for STAT3 was shown previously for the regulation of *FAS* (37) and *p53* (43) transcription, whereas STAT3,

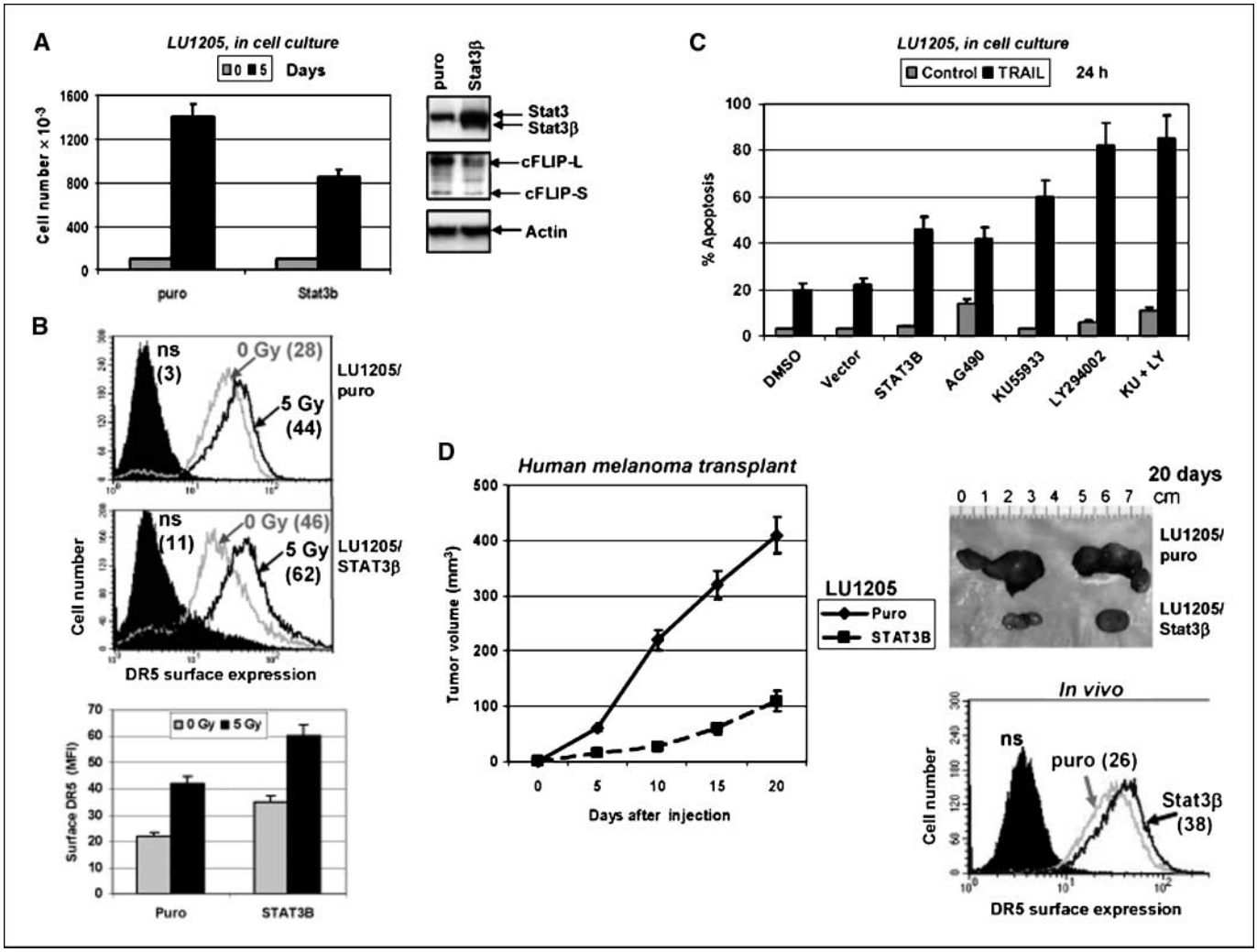

Figure 6. Effects of dominant-negative STAT3β on DR5 surface expression in cell culture and in melanoma transplant in nude mice. *A,* cell culture growth of LU1205-puro and LU1205-STAT3β cells transfected with the empty vector pBabe-puro or with STAT3β construct. Western blotting showed levels of STAT3β. *B,* surface expression of DR5 on LU1205-puro and LU1205-STAT3β cells in culture before and after γ-irradiation. *Top,* results of typical experiment. *Columns,* mean; *bars,* SD. *C,* apoptosis induced by TRAIL (50 ng/mL) in the control LU1205-puro and LU1205-STAT3β cells as well as by TRAIL in combination with AG490 (50 μmol/L), KU-55933 (10 μmol/L), or LY294002 (LY; 50 μmol/L) in LU1205 cells. *Columns,* mean; *bars,* SD ($P < 0.05$, Student's *t* test). *D,* LU1205-puro and LU1205-STAT3β melanoma transplant growth in nude mice. Melanoma cells were injected subcutaneously into athymic nude mice, and tumor volume was monitored during the next 3 wk. Surface expression of DR5 on LU1205-puro and LU1205-STAT3β cells *in vivo* was determined by fluorescence-activated cell sorting analysis.

together with NF-κB, was involved in the positive control of antiapoptotic *Bcl-xL* and *cFLIP/CFLAR* gene expression (44–47). Coordinated up-regulation of DR5 expression (through suppression of ATM-STAT3 activity) and down-regulation of cFLIP protein levels (through suppression of ATM-NF-κB- and ATM-STAT3-dependent expression) may represent an efficient combination treatment that can dramatically accelerate TRAIL-mediated apoptosis in several cancer cell systems (26, 46).

One of the critical factors that determine the efficacy of anticancer therapy is the ability to selectively kill cancer cells while minimally affecting normal cells. In this context, TRAIL via interaction with the correspondent TRAIL-R1/R2 on the surface of cancer cells may induce a fatal signaling cascade in cancer cells and has only minimal cytotoxic effects in normal cells (10). There have been numerous attempts to increase sensitivity of cancer cells to TRAIL using different types of combined treatment. Based on the results of the present study, combined treatment with γ-irradiation and an ATM inhibitor that is followed by treatment with exogenous TRAIL represents a potentially effective approach for cancer cell killing. Our findings provide a basis for further investigation of TRAIL-mediated target treatment to overcome apoptotic resistance of metastatic melanomas.

Disclosure of Potential Conflicts of Interest

No potential conflicts of interest were disclosed.

Acknowledgments

Received 10/7/08; revised 1/30/09; accepted 2/12/09; published OnlineFirst 4/7/09.

Grant support: NIH grant CA 49062, Superfund grant ES 10349, and Environmental Center grant ES 09059.

The costs of publication of this article were defrayed in part by the payment of page charges. This article must therefore be hereby marked *advertisement* in accordance with 18 U.S.C. Section 1734 solely to indicate this fact.

We thank Drs. Y. Shiloh, Z. Ronai, M. Herlyn, A. Balajee, and H.B. Lieberman for plasmid constructs, melanoma lines, and discussion.

References

1. Shiloh Y. The ATM-mediated DNA-damage response: taking shape. Trends Biochem Sci 2006;31:402–10.
2. Barlow C, Hirotsune S, Paylor R, et al. Atm-deficient mice: a paradigm of ataxia telangiectasia. Cell 1996;86: 159–71.
3. Matsuoka S, Ballif BA, Smogorzewska A, et al. ATM and ATR substrate analysis reveals extensive protein networks responsive to DNA damage. Science 2007;316:1160–6.
4. Wu ZH, Shi Y, Tibbetts RS, Miyamoto S. Molecular linkage between the kinase ATM and NF-κB signaling in response to genotoxic stimuli. Science 2006;311:1141–6.
5. Bhoumik A, Takahashi S, Breitweiser W, Shiloh Y, Jones N, Ronai Z. ATM-dependent phosphorylation of ATF2 is required for the DNA damage response. Mol Cell 2005; 18:577–87.
6. Zhang Y, Cho YY, Petersen BL, Bode AM, Zhu F, Dong Z. Ataxia telangiectasia mutated proteins, MAPKs, and RSK2 are involved in the phosphorylation of STAT3. J Biol Chem 2003;278:12650–9.
7. Perlis C, Herlyn M. Recent advances in melanoma biology. Oncologist 2004;9:182–7.
8. Ashkenazi A. Targeting death and decoy receptors of the tumour-necrosis factor superfamily. Nat Rev Cancer 2002;2:420–30.
9. Schaefer U, Voloshanenko O, Willen D, Walczak H. TRAIL: a multifunctional cytokine. Front Biosci 2007;12: 3813–24.
10. Ashkenazi A, Herbst RS. To kill a tumor cell: the potential of proapoptotic receptor agonists. J Clin Invest 2008;118:1979–90.
11. Chinnaiyan AM, Prasad U, Shankar S, et al. Combined effect of tumor necrosis factor-related apoptosis-inducing ligand and ionizing radiation in breast cancer therapy. Proc Natl Acad Sci U S A 2000;97:1754–9.
12. Ivanov VN, Zhou H, Hei TK. Sequential treatment by ionizing radiation and sodium arsenite dramatically accelerates TRAIL-mediated apoptosis of human melanoma cells. Cancer Res 2007;67:5397–407.
13. Ashkenazi A, Holland P, Eckhardt SG. Ligand-based targeting of apoptosis in cancer: the potential of recombinant human apoptosis ligand 2/tumor necrosis factor-related apoptosis-inducing ligand (rhApo2L/ TRAIL). J Clin Oncol 2008;26:3621–30.
14. Satyamoorthy K, DeJesus E, Linnenbach AJ, et al. Melanoma cell lines from different stages of progression and their biological and molecular analyses. Melanoma Res 1997;7 Suppl 2:S35–42.
15. van Dam H, Huguier S, Kooistra K, et al. Autocrine growth and anchorage independence: two complementing Jun-controlled genetic programs of cellular transformation. Genes Dev 1998;12:1227–39.
16. Takimoto R, El-Deiry WS. Wild-type p53 transactivates the KILLER/DR5 gene through an intronic sequence-specific DNA-binding site. Oncogene 2000;19:1735–43.
17. Bartke T, Siegmund D, Peters N, et al. p53 upregulates cFLIP, inhibits transcription of NF-κB-regulated genes and induces caspase-8-independent cell death in DLD-1 cells. Oncogene 2001;20:571–80.
18. Ricci MS, Jin Z, Dews M, et al. Direct repression of FLIP expression by c-myc is a major determinant of TRAIL sensitivity. Mol Cell Biol 2004;24:8541–55.
19. Resnick-Silverman L, St Clair S, Maurer M, Zhao K, Manfredi JJ. Identification of a novel class of genomic DNA-binding sites suggests a mechanism for selectivity in target gene activation by the tumor suppressor protein p53. Genes Dev 1998;12:2102–7.
20. Biton S, Dar I, Mittelman L, Pereg Y, Barzilai A, Shiloh Y. Nuclear ataxia-telangiectasia mutated (ATM) mediates the cellular response to DNA double strand breaks in human neuron-like cells. J Biol Chem 2006;281: 17482–91.
21. Ivanov VN, Hei TK. Arsenite sensitizes human melanomas to apoptosis via tumor necrosis factor α-mediated pathway. J Biol Chem 2004;279:22747–58.
22. Bakkenist CJ, Kastan MB. DNA damage activates ATM through intermolecular autophosphorylation and dimer dissociation. Nature 2003;421:499–506.
23. Hirao A, Kong YY, Matsuoka S, et al. DNA damage-induced activation of p53 by the checkpoint kinase Chk2. Science 2000;287:1824–7.
24. Ivanov VN, Partridge MA, Johnson GE, Huang SX, Zhou H, Hei TK. Resveratrol sensitizes melanomas to TRAIL through modulation of antiapoptotic gene expression. Exp Cell Res 2008;314:1163–76.
25. Thayaparasingham B, Kunz A, Peters N, Kulms D. Sensitization of melanoma cells to TRAIL by UVB-induced and NF-κB-mediated downregulation of XIAP. Oncogene 2009;28:345–62.
26. Ivanov VN, Hei TK. Sodium arsenite accelerates TRAIL-mediated apoptosis in melanoma cells through upregulation of TRAIL-R1/R2 surface levels and down-regulation of cFLIP expression. Exp Cell Res 2006;312: 4120–38.
27. Amundson SA, Do KT, Vinikoor LC, et al. Integrating global gene expression and radiation survival parameters across the 60 cell lines of the National Cancer Institute Anticancer Drug Screen. Cancer Res 2008;68: 415–24.
28. Rashi-Elkeles S, Elkon R, Weizman N, et al. Parallel induction of ATM-dependent pro- and antiapoptotic signals in response to ionizing radiation in murine lymphoid tissue. Oncogene 2006;25:1584–92.
29. Hickson I, Zhao Y, Richardson CJ, et al. Identification and characterization of a novel and specific inhibitor of the ataxia-telangiectasia mutated kinase ATM. Cancer Res 2004;64:9152–9.
30. Ito K, Nakazato T, Miyakawa Y, Yamato K, Ikeda Y, Kizaki M. Caffeine induces G_2/M arrest and apoptosis via a novel p53-dependent pathway in NB4 promyelocytic leukemia cells. J Cell Physiol 2003;196:276–83.
31. Shetty S, Graham BA, Brown JG, et al. Transcription factor NF-κB differentially regulates death receptor 5 expression involving histone deacetylase 1. Mol Cell Biol 2005;25:5404–16.
32. Ravi R, Bedi GC, Engstrom LW, et al. Regulation of death receptor expression and TRAIL/Apo2L-induced apoptosis by NF-κB. Nat Cell Biol 2001;3:409–16.
33. Higuchi H, Grambihler A, Canbay A, Bronk SF, Gores GJ. Bile acids up-regulate death receptor 5/TRAIL-receptor 2 expression via a c-Jun N-terminal kinase-dependent pathway involving Sp1. J Biol Chem 2004;279: 51–60.
34. Wen Z, Zhong Z, Darnell JE, Jr. Maximal activation of transcription by Stat1 and Stat3 requires both tyrosine and serine phosphorylation. Cell 1995;82:241–50.
35. Kusaba M, Nakao K, Goto T, et al. Abrogation of constitutive STAT3 activity sensitizes human hepatoma cells to TRAIL-mediated apoptosis. J Hepatol 2007;47: 546–55.
36. Meng RD, El-Deiry WS. p53-independent up-regulation of KILLER/DR5 TRAIL receptor expression by glucocorticoids and interferon-γ. Exp Cell Res 2001;262:154–69.
37. Ivanov VN, Bhoumik A, Krasilnikov M, et al. Cooperation between STAT3 and c-Jun suppresses Fas transcription. Mol Cell 2001;7:517–28.
38. Ivanov VN, Krasilnikov M, Ronai Z. Regulation of Fas expression by STAT3 and c-Jun is mediated by phosphatidylinositol 3-kinase-AKT signaling. J Biol Chem 2002;277:4932–44.
39. Truman JP, Gueven N, Lavin M, et al. Down-regulation of ATM protein sensitizes human prostate cancer cells to radiation-induced apoptosis. J Biol Chem 2005;280:23262–72.
40. Rainey MD, Charlton ME, Stanton RV, Kastan MB. Transient inhibition of ATM kinase is sufficient to enhance cellular sensitivity to ionizing radiation. Cancer Res 2008;68:7466–74.
41. O'Connor MJ, Martin NM, Smith GC. Targeted cancer therapies based on the inhibition of DNA strand break repair. Oncogene 2007;26:7816–24.
42. Leslie K, Lang C, Devgan G, et al. Cyclin D1 is transcriptionally regulated by and required for transformation by activated signal transducer and activator of transcription 3. Cancer Res 2006;66:2544–52.
43. Niu G, Wright KL, Ma Y, et al. Role of Stat3 in regulating p53 expression and function. Mol Cell Biol 2005;25:7432–40.
44. Tsukahara T, Kannagi M, Ohashi T, et al. Induction of Bcl-x(L) expression by human T-cell leukemia virus type 1 Tax through NF-κB in apoptosis-resistant T-cell transfectants with Tax. J Virol 1999;73:7981–7.
45. Catlett-Falcone R, Landowski TH, Oshiro MM, et al. Constitutive activation of Stat3 signaling confers resistance to apoptosis in human U266 myeloma cells. Immunity 1999;10:105–15.
46. Fulda S, Debatin KM. Extrinsic versus intrinsic apoptosis pathways in anticancer chemotherapy. Oncogene 2006;25:4798–811.
47. Haga S, Terui K, Zhang HQ, et al. Stat3 protects against Fas-induced liver injury by redox-dependent and -independent mechanisms. J Clin Invest 2003;112: 989–98.